High repetition rate passively *Q*-switched laser on Nd:SRA at 1049 nm with MXene $Ti_3C_2T_x$

Mengfei Zhao (赵梦菲)[1], Zhongmian Zhang (张中勉)[1], Xiaoyue Feng (冯潇玥)[1], Mengyu Zong (宗梦雨)[1], Jie Liu (刘 杰)[1,*], Xiaodong Xu (徐晓东)[2], and Han Zhang (张 晗)[3]

[1]*Shandong Provincial Engineering and Technical Center of Light Manipulations & Shandong Provincial Key Laboratory of Optics and Photonic Device, School of Physics and Electronics, Shandong Normal University, Jinan 250358, China*

[2]*Jiangsu Key Laboratory of Advanced Laser Materials and Devices, School of Physics and Electronic Engineering, Jiangsu Normal University, Xuzhou 221116, China*

[3]*Key Laboratory of Optoelectronic Devices and Systems of Ministry of Education and Guangdong Province, College of Electronic Science and Technology and College of Optoelectronics Engineering, Shenzhen University, Shenzhen 518060, China*

**Corresponding author: jieliu@sdnu.edu.cn*

Received November 13, 2019; accepted December 19, 2019; posted online April 3, 2020

A new disordered crystal Nd:$SrAl_{12}O_{19}$ (Nd:SRA) with an Nd^{3+} doping concentration of 5% was successfully grown using the Czochralski method. A diode-pumped Nd:SRA *Q*-switched laser operating at 1049 nm was demonstrated for the first time, to the best of our knowledge. Based on an MXene $Ti_3C_2T_x$ sheet, a high repetition rate of 201 kHz and a *Q*-switched pulse width of 346 ns were obtained when the absorbed pump power was 2.8 W. The peak power and single pulse energy were 1.87 W and 0.65 μJ, respectively.

Keywords: Nd:$SrAl_{12}O_{19}$ crystal; MXene $Ti_3C_2T_x$; disordered crystal; passively Q-switched lasers.
doi: 10.3788/COL202018.041401.

High repetition rate passively *Q*-switched solid-state lasers in the 1 μm band have many areas of application such as industrial manufacturing, laser communication, laser processing, and medical treatment[1,2]. The laser gain medium is an important factor for *Q*-switched pulse lasers. To date, Nd^{3+}-doped laser crystals are the most typically and widely used laser gain media in the 1 μm band[3–6]. However, their relatively narrow emission bandwidth has limited their advancement in short-pulse generation, so new laser crystals with excellent properties are increasingly being explored[7–9].

Recently, attention has been drawn to a new disordered oxide crystal, $SrAl_{12}O_{19}$ (SRA), which is a common phosphor material[10]. Nowadays, rare-earth-ion-doped SRAs have shown great performance in the laser field[11–14]. The SRA has a light transmission band of 0.2–5.8 μm. In an Nd:SRA crystal, the Nd^{3+} fluorescence lifetime of $^4F_{3/2}$ energy level is about 400 μs[15]. This is much longer than that of other Nd^{3+}-doped laser crystals, which means that it can store more energy[16,17]. Compared to other Nd^{3+}-doped disordered laser gain media[18–20], the large distribution coefficient (>0.6) of Nd^{3+} guarantees its higher gain[15]. Moreover, the large thermal diffusivity, high damage threshold, and non-uniform broadening of the emission spectrum caused by the disordered structure of the crystal make it a potential ultra-short laser gain medium[21–24]. It is worth noting that the output wavelength of the laser on Nd:SRA is 1049 nm, owing to the $^4F_{3/2}$–$^4I_{11/2}$ energy level transition of Nd^{3+} in SRA. In recent research on laser performance, rare-earth ions based on SRA include Pr^{3+}, Mg^{2+}, Sm^{3+}, etc.[11,25]. However, studies related to the laser characteristics of the Nd:SRA crystal have not been reported until now.

A saturable absorber is another significant factor in passively *Q*-switched technology[26–28]. The new much-debated, two-dimensional material MXenes have the outstanding optical characteristics such as high damage threshold, fast recovery, and large non-linear absorption coefficient[29,30]. They have been used as *Q*-switched components in many passively *Q*-switched laser experiments involving multiple wavebands[31–33]. In experiments, MXenes are usually fabricated by the acid etching process.

In this Letter, a stable passively *Q*-switched operation on Nd:SRA has been demonstrated for the first time, to the best of our knowledge. Using an MXene $Ti_3C_2T_x$ sheet, a repetition rate as high as 201 kHz with the corresponding pulse width of 346 ns was obtained. The single pulse energy and peak power were 0.65 μJ and 1.87 W, respectively. Detailed aspects of Nd:SRA laser performance are discussed below.

The MXene $Ti_3C_2T_x$ solution in our experiment was prepared by chemical acid etching technology[34] and by smearing the solution at quartz substrates via the spin coater with a low speed of 1000 r/s to distribute the material evenly. The finished sample sheet was then placed horizontally at the normal temperature to dry. The scanning electron microscopy (SEM) image in Fig. 1(a) shows that it has a lamellar graphene-like structure. We characterized a Z-scan transmittance curve by using a

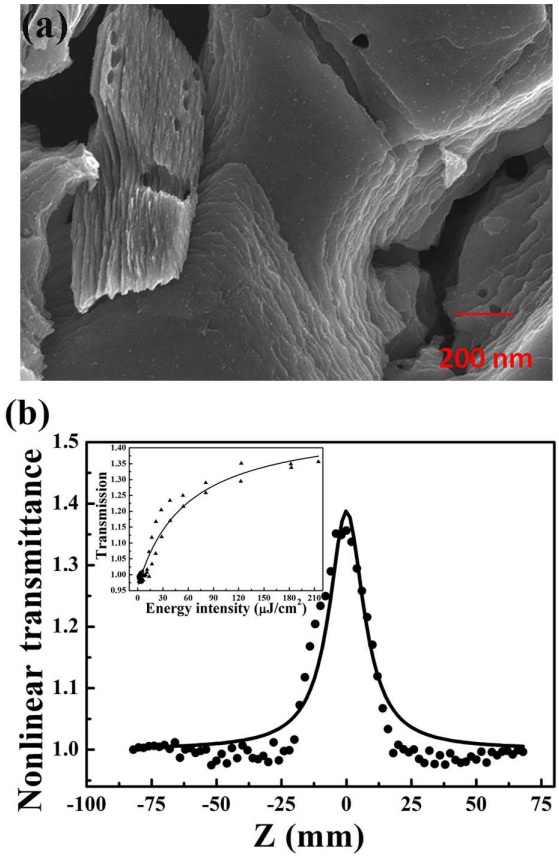

Fig. 1. (a) SEM image of MXene $Ti_3C_2T_x$, (b) Z-scan curve of MXene $Ti_3C_2T_x$, and non-linear transmission versus energy intensity.

Z-scan non-linear optical measurement system, presented in Fig. 1(b). The insert shows the non-linear transmittance versus energy intensity. The saturation optical intensity and modulation depth were 107 μJ/cm^2 and 36.7%, respectively. The results were fitted with the saturable absorber model, given by[35]

$$T(z) = 1 - \frac{\beta I_0 L_{\text{eff}}}{2\sqrt{2}(1 + z^2/z_0^2)}, \tag{1}$$

where $T(z)$ is the normalized transmittance, z is the position of the sample relative to the focus, I_0 is the on-axis peak intensity at focus, z_0 is the Rayleigh range, $L_{\text{eff}} = (1 - e^{-\alpha L})/\alpha$ is the effective length, and L is the length of the sample.

The experimental device is shown in Fig. 2. A 30 W commercial fiber-coupled laser diode emitting at 808 nm with a numerical aperture (NA) of 0.22 and a core diameter of 200 μm was used as the pumping source. The pump light was coupled into the Nd:SRA crystal by the optical collimation system of 1:1. The Nd:SRA (5 at.%) crystal was cut along its c axis, polished with the parallel end surface, and uncoated. The dimensions of the crystal were 3 mm × 3 mm × 6 mm. The crystal was wrapped with indium foil and tightly mounted on a water-cooled copper heat sink at a temperature of 16°C.

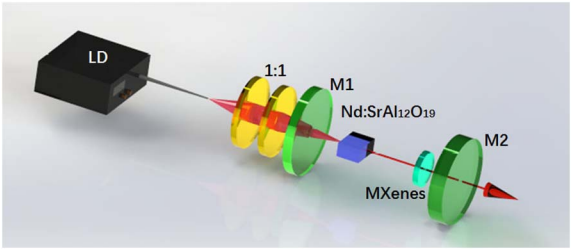

Fig. 2. Experimental setup of the Q-switched laser.

In order to study the properties of the crystal, we designed a simple laser resonator consisting of an input plane mirror (M1) and a concave output mirror (M2). M1 was high-transmission (HT) coated at 808 nm and high-reflection (HR) coated at 1064 nm. M2 had a radius of 100 mm and was coated with a transmission of 3% at 1064 nm. To obtain the best state of the cavity resonator, we calculated the optimum cavity length of 36 mm using the ABCD matrix propagation theory. The mode radius at the MXenes $Ti_3C_2T_x$ sheet was computed to be 114 μm.

By replacing M2 with different transmittances, we found that the output mirrors with transmission of 3% showed better performance of the laser. By optimizing the cavity type and cavity length, the saturable absorber MXene $Ti_3C_2T_x$ film was then inserted into the resonant cavity, close to M2. After carefully adjusting the position of the absorber and the cavity, a passively Q-switched pulse train appeared in the oscilloscope (Tektronix DPO-4104, USA) at an absorbed pump power of 2.29 W. The output power increased with the increase of the pump power. Under an absorbed pump power of 2.8 W, the laser had a maximum average output power of 130 mW, as plotted in Fig. 3. Owing to the insertion of the uncoated absorber, which led to much loss in the cavity, the maximum output power was not too high. It was obvious that there was no saturation trend of the laser output power. In order to protect the crystal and absorber, no further pump power was added in the Q-switched operation. By optimizing the parameters of MXene $Ti_3C_2T_x$ and processing the crystal with an anti-reflection coating, an

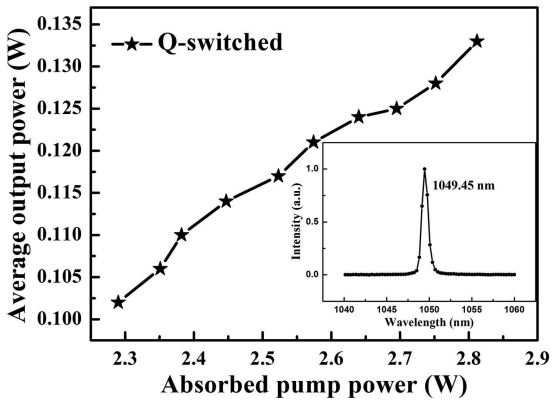

Fig. 3. Average output power of the Q-switched Nd:SRA laser and spectrum of the passively Q-switched laser at 1049 nm.

improvement in the Q-switched output power was expected. By using a spectrometer (Avaspec-3648-USB2), we can see that the center wavelength was 1049.45 nm, and the full width at half-maximum (FWHM) was 0.8 nm, as shown in the insert of Fig. 3.

Figure 4(a) illustrates the dependence of both the pulse width and the repetition rate on the absorbed pump power. With the increase of pump power, the repetition rate varied from 134 to 201 kHz. The pulse width gradually shortened, and its minimum pulse width was 346 ns, as the absorbed pump power was 2.8 W. Using the formulas $E = P_{\text{ave}}/f$ and $P_{\text{peak}} = E/\tau$, where P_{ave} is the average output power, τ is the pulse width, f is the repetition frequency, E is the single pulse energy, and P_{peak} is the peak power, we calculated the highest single pulse energy and peak power as 0.65 μJ and 1.87 W, respectively, as displayed in Fig. 4(b). The output pulse energy increases with the increase of pump power, which is caused by the thermal lensing effect.

A typical Q-switched pulse train was observed at 10 μs/div and 400 ns/div using a Tektronix DPO4104 digital oscilloscope, as shown in Fig. 5(a). The pulse contours were asymmetrical, with fast-rising and slow-falling edges; this was mainly due to the saturable absorption characteristics of MXene $Ti_3C_2T_x$. Moreover, by using an M^2 factor analyzer (Spiricon-M^2-200S-USB), the spatial

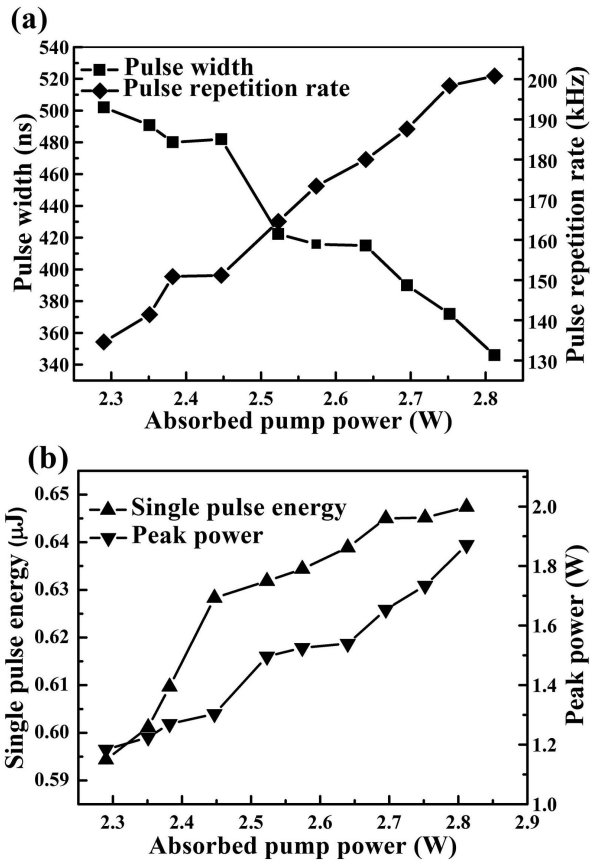

Fig. 4. (a) Pulse duration and repetition rate dependence on the absorbed pump power, (b) single pulse energy and peak power versus the absorbed pump power.

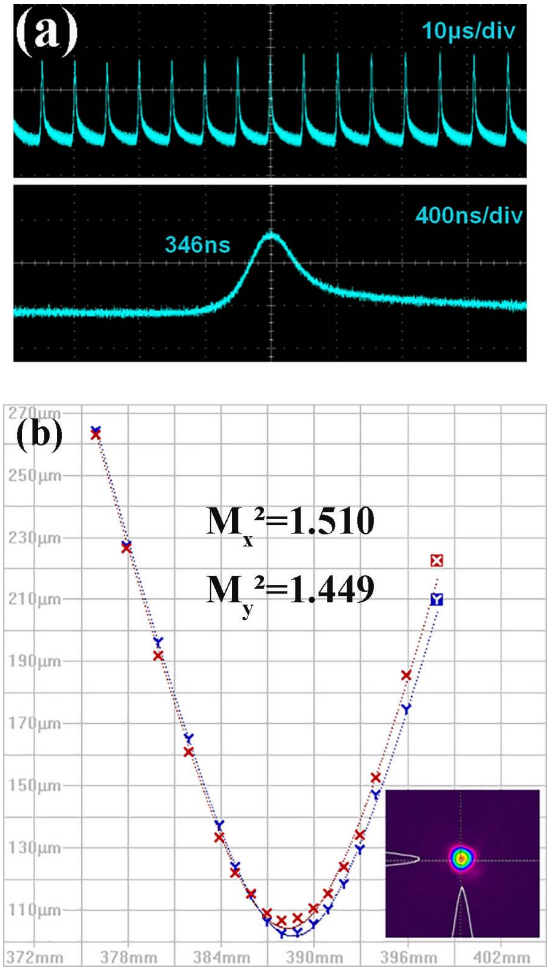

Fig. 5. (a) Typical pulse profiles on time scales of 10 μs/div and 400 ns/div, (b) spatial beam profile and beam quality of the Q-switched laser.

beam profile and laser beam quality were observed at a maximum average output power, as shown in Fig. 5(b). The relatively small M^2 value ($M_x^2 = 1.510$, $M_y^2 = 1.449$) and the symmetric hyperbolic function indicated that the laser was operating under a nearly Gaussian mode.

In this work, the nanosecond high repetition rate Q-switched laser on Nd:SRA was demonstrated for the first time, to the best of our knowledge, at 1049.45 nm. With an MXene $Ti_3C_2T_x$ sheet, a clean pulse laser with a maximum repetition rate of 201 kHz was achieved. The minimum pulse duration was 346 ns, corresponding to the single pulse energy of 0.65 μJ and peak power of 1.87 W. The combination of Nd:SRA and MXenes $Ti_3C_2T_x$ proved a feasible approach to achieve a high repetition rate laser. However, we found that the strong nonuniform broadening absorption and emission spectra make Nd:SRA a promising ultra-short laser gain medium, so we suggest that the ultra-fast laser characteristic of Nd:SRA needs to be further explored. By optimizing the optical quality of the Nd:SRA crystal and designing a suitable laser cavity, ultra-fast laser operation of the Nd:SRA crystal is expected.

This work was supported by the National Natural Science Foundation of China (NSFC) (No. 11974220).

References

1. D. M. Boroson, B. S. Robinson, D. V. Murphy, D. A. Burianek, F. Khatri, J. M. Kovalik, Z. Sodnik, and D. M. Cornwell, Proc. SPIE **8971**, 89710S (2014).
2. N. P. Y. Chan, S. G. Y. Ho, S. Y. N. Shek, C. K. Yeung, and H. H. Chan, Lasers Surg. Med. **42**, 712 (2010).
3. N. Pavel, M. Tsunekane, and T. Taira, Opt. Express **19**, 9378 (2011).
4. Q. Q. Hao, S. Y. Pang, J. Liu, and L. B. Su, Appl. Opt. **57**, 6491 (2018).
5. Y. J. Wu, S. Y. Pang, Y. Q. Zu, Q. Q. Peng, J. M. Yang, J. Liu, and L. B. Su, Chin. Opt. Lett. **16**, 020015 (2018).
6. Y. J. Wu, C. Zhang, J. J. Liu, H. N. Zhang, J. M. Yang, and J. Liu, Opt. Laser Technol. **97**, 268 (2017).
7. T. J. Wang, J. Wang, Y. G. Wang, X. G. Yang, S. C. Liu, R. D. Lü, and Z. D. Chen, Chin. Opt. Lett. **17**, 020009 (2019).
8. C. Li, W. Cai, J. Liu, L. B. Su, D. P. Jiang, F. K. Ma, Q. Zhang, J. Xu, and Y. G. Wang, Opt. Commun. **372**, 76 (2016).
9. Q. Z. Qian, N. Wang, S. Z. Zhao, G. Q. Li, T. Li, D. C. Li, K. J. Yang, J. Zang, and H. Y. Ma, Chin. Opt. Lett. **17**, 041401 (2019).
10. J. M. P. J. Verstegen, J. Electrochem. Soc. **121**, 1623 (1974).
11. D. T. Marzahl, F. Reichert, B. Stumpf, P. W. Metz, C. Kraenkel, and G. Huber, in *Conference on Lasers & Electro-Optics* (2014), paper SM3F.2.
12. F. Reichert, D. T. Marzahl, P. Metz, M. Fechner, N. O. Hansen, and G. Huber, Opt. Lett. **37**, 4889 (2012).
13. M. Fechner, F. Reichert, N. O. Hansen, K. Petermann, and G. Huber, Appl. Phys. B **102**, 731 (2011).
14. D. Merkle, B. Zandi, R. Moncorge, Y. Guyot, and H. R. Verdun, J. Appl. Phys. **79**, 1849 (1997).
15. K. S. Bagdasarov, A. A. Kaminskii, A. M. Kevorkov, L. Li, A. M. Prokhorov, S. É. Sarkisov, and T. A. Tevosyan, Sov. Phys. Dokl. **19**, 350 (1974).
16. H. Tajalli, in *International Quantum Electronics Conference* (1986), paper WGG8.
17. P. Zeller and P. Peuser, Opt. Lett. **25**, 34 (2000).
18. H. H. Yu, H. J. Zhang, Z. P. Wang, J. Y. Wang, Y. G. Yu, Z. B. Shi, X. Y. Zhang, and M. H. Jiang, Opt. Lett. **34**, 151 (2009).
19. Y. G. Yu, J. Y. Wang, H. J. Zhang, Z. P. Wang, H. H. Yu, and M. H. Jiang, Opt. Lett. **34**, 467 (2009).
20. H. H. Yu, Y. G. Yu, H. J. Zhang, Z. P. Wang, J. Y. Wang, X. F. Cheng, Z. S. Shao, and M. H. Jiang, J. Cryst. Growth **293**, 394 (2006).
21. H. R. Verdun, D. E. Wortman, C. A. Morrison, and J. L. Bradshaw, Opt. Mater. **7**, 117 (1997).
22. Y. X. Pan, S. D. Zhou, J. W. Wang, B. Xu, J. Liu, Q. S. Song, J. Xu, D. Z. Li, L. Peng, X. D. Xu, and J. Xu, Appl. Opt. **57**, 9657 (2018).
23. W. L. Tian, C. Yu, J. F. Zhu, D. C. Zhang, Z. Y. Wei, X. D. Xu, and J. Xu, Opt. Express **27**, 21448 (2019).
24. Z. Tian, B. Wang, C. Gao, Q. Wu, X. Xu, J. Xu, and B. Zhang, J. Russ. Laser Res. **40**, 94 (2019).
25. D. T. Marzahl, F. Reichert, P. W. Metz, M. Fechner, N. O. Hansen, and G. Huber, Appl. Phys. B **116**, 109 (2014).
26. Z. Q. Li, Y. X. Zhang, C. Chen, H. H. Yu, and C. Feng, Opt. Express **26**, 11321 (2018).
27. Z. Q. Li, R. Li, C. Pang, N. N. Dong, J. Wang, H. H. Yu, and F. Chen, Opt. Express **27**, 8727 (2019).
28. Q. Y. Hu, X. Y. Zhang, Z. J. Liu, P. Li, M. Li, Z. H. Cong, Z. G. Qin, and X. H. Chen, Opt. Laser Technol. **119**, 105639 (2019).
29. Q. M. Peng, J. X. Guo, Q. R. Zhang, J. Y. Xiang, B. Z. Liu, A. G. Zhou, R. P. Liu, and Y. J. Tian, J. Am. Chem. Soc. **136**, 4113 (2014).
30. X. L. Sun, B. T. Zhang, B. Z. Yan, G. R. Li, H. K. Nie, K. J. Yang, C. Q. Zhang, and J. L. He, Opt. Lett. **43**, 3862 (2018).
31. Y. Q. Zu, C. Zhang, X. S. Guo, W. Y. Liang, J. Liu, L. B. Su, and H. Zhang, Laser Phys. Lett. **16**, 015803 (2018).
32. C. Wang, Q. Q. Peng, X. W. Fan, W. Y. Liang, F. Zhang, J. Liu, and H. Zhang, Chin. Phys. B **27**, 094214 (2018).
33. Q. Q. Hao, J. J. Liu, Z. Zhang, B. Zhang, F. Zhang, J. M. Yang, J. Liu, L. B. Su, and H. Zhang, Appl. Phys. Express **12**, 085506 (2019).
34. K. Hantanasirisakul, M. Q. Zhao, P. Urbankowski, J. Halim, B. Anasori, S. Kota, C. E. Ren, M. W. Barsoum, and Y. Gogotsi, Adv. Electron. Mater. **2**, 1600050 (2016).
35. S. B. Lu, L. L. Miao, Z. N. Guo, X. Qi, C. J. Zhao, H. Zhang, S. C. Wen, D. Y. Tang, and D. Y. Fan, Opt. Express **23**, 11183 (2015).